COURSE 7

"BURGULENCE"

U. FRISCH and J. BEC

Laboratoire G.D. Cassini, UMR 6529,
Observatoire de la Côte d'Azur,
BP. 4229, 06304 Nice Cedex 4, France

Contents

"BURGULENCE"

U. Frisch and J. Bec

1 Introduction

These lectures are about the d-dimensional Burgers equation

$$\partial_t \mathbf{v} + (\mathbf{v} \cdot \nabla)\, \mathbf{v} = \nu \nabla^2 \mathbf{v}, \qquad \mathbf{v} = -\nabla \psi. \tag{1.1}$$

Note that the constraint that $\mathbf{v}$ be derived from a (velocity) potential ψ is trivially satisfied if $d = 1$. The word "burgulence", as we use it here, is a contraction of "Burgers" and "turbulence". It means "the study of random solutions to the Burgers equation". The randomness may arise because random initial conditions $\mathbf{v}_0 = -\nabla \psi_0$ are given or because a random driving force $\mathbf{f} = -\nabla F$ is added to the r.h.s. of (1.1), or both. When $\mathbf{f} = 0$ one speaks about "decaying burgulence".

In the thirties when the Dutch scientist J.M. Burgers introduced the equation in the one-dimensional case, he hoped to contribute to the study of turbulence with a simple model which, obviously, has a lot in common with the Navier–Stokes equation:

- same type of advective nonlinearity;
- presence of a diffusion term from which a Reynolds number may be defined;
- many invariance and conservation laws in common: invariance under translations in space and time, parity invariance, conservation of momentum and energy (only for $\nu = 0$ and $d = 1$).

Such hopes appeared to be shattered when, in the fifties, Hopf [1] and Cole [2] discovered – some say rediscovered – that the Burgers equation can actually be integrated explicitly (we shall return to this matter later). Indeed, an important property of the Navier–Stokes equation, not shared by the Burgers equation, is the sensitivity to small changes in the initial conditions in the presence of boundaries or driving forces and at sufficiently

high Reynolds numbers. Hence, the Burgers equation is not a good model for one of the most important aspects of turbulence: the spontaneous arise of randomness by chaotic dynamics.

In spite of this there has been a strong renewal of interest in the Burgers equation, starting in the eighties, for a variety of reasons which we shall now explain. As a quantitative measure of the current interest, Table 1 shows some web-based statistical figures on the number of hits as of August 2000 (Google is an all-purpose search engine and "Los Alamos" stands for the nlin (ex-chao-dyn) preprint archive): the Burgers equation, which obviously describes a compressible flow (in one dimension there exist only trivial incompressible flows), has found many applications in *nonlinear acoustics* and other nonlinear wave problems. A review may be found in reference [3].

Table 1. Web-based statistical data.

	Navier–Stokes equation	Burgers equation
Google	15 000	4000
Los Alamos	100	75

1.1 The Burgers equation in cosmology

The Burgers equation has found interesting applications in cosmology, where it is known, in one instance, as the "Zel'dovich approximation" [4] and, in another instance, as the "adhesion model" [5]. Here, we shall give a brief introduction to how the Burgers equation arises in cosmology. More details may be found in [6–9]. Just after the baryon-photon decoupling in the early Universe, there may have been a rarefied medium formed by collisionless dustlike particles without pressure, interacting only *via* Newtonian gravity [8]. The gravitational potential is then determined from the fluctuations in mass density by a Poisson equation. Limiting ourselves to the case of a single type of matter, we can schematically write the acceleration of a fluid particle as follows:

acceleration =	pressure term	+	viscous term	+	expansion term	+	gravit. term
$\partial_t \mathbf{v} + \mathbf{v} \cdot \nabla \mathbf{v}$	negligible		?		$\propto \mathbf{v}$ in comov. coord.		

On the left hand side (l.h.s.) we recognize the familiar terms of the Burgers equation. The pressure is usually neglected because the matter is very cold. We shall come back to the viscous term later. The expansion term,

proportional to the velocity, arises because the equation is written in a frame comoving with the expansion of the Universe.

It turns out that when the problem of self-gravitating gas in an expanding universe is examined in the linear approximation (small density fluctuations) an instability is obtained in which the dominant mode has the following properties [8, 9]:

- it is potential ($\mathbf{v} = -\nabla\psi$);
- the expansion and gravitational terms cancel.

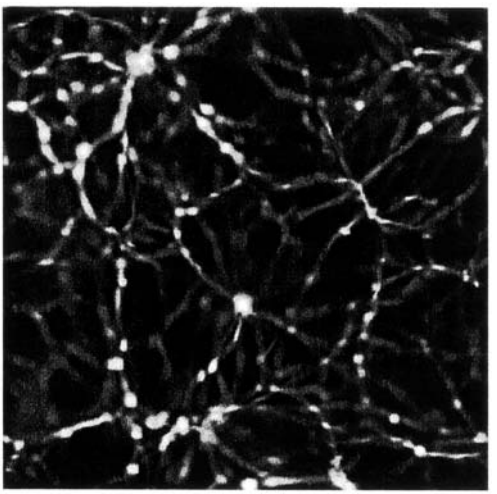

Fig. 1. N-body simulation by the Virgo Consortium (see `http://star-www.dur.ac.uk/~frazerp/virgo/virgo.html`). The simulation has 256^3 particles and was done on two large Cray T3D parallel supercomputers at the computing centers Garching (D) and Edinburgh (GB). The brightness is proportional to the log of the density of the particles.

In 1970, Zel'dovich [4] proposed to extend these properties into the nonlinear regime where density fluctuations become strong and mass condensation forming large-scale structures appear. Furthermore, this "Zel'dovich approximation" is exact in one dimension, irrespective of the strength of fluctuations. Clearly, in the Zel'dovich approximation each fluid particle is just moving in a straight line with constant velocity (after a suitable nonlinear change of variable of the time). Just like a family of straight light rays forms generally caustics along which the intensity is infinite, the material particle lines form singular objects along which the mass density is infinite.

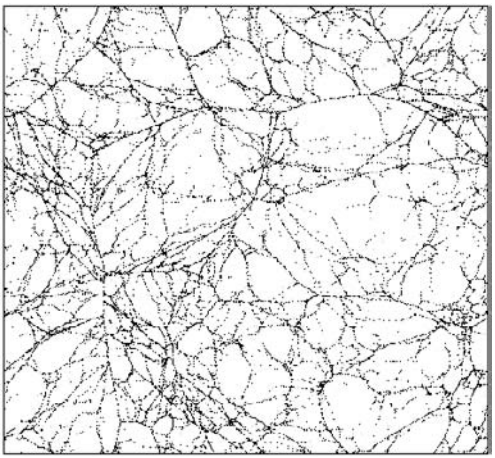

Fig. 2. Mass density field from a 512^2 simulation of the Burgers equation with random scale-free initial data (from Ref. [7]).

Arnold *et al.* [10] studied the various kind of singularities which can form in this way, to see if they could account for known large-scale structures such as galaxies and clusters. Observations and numerical simulations have now revealed that large-scale structures are much simpler than the mathematical objects generated in a caustic-type theory.

Consider for example Figure 1 which shows a thin slice of a simulated universe using the so-called ΛCDM model (cold dark matter with cosmological constant). The line-like and node-like features on this slice are actually sheets and filaments embedded in the three-dimensional space. Sheets (walls), filaments and nodes (clusters) are the most common structures observed in such simulations. As was shown by Gurbatov and Saichev [5] these are precisely the structures obtained if one modifies the Zel'dovich approximation by requiring that particles should not cross but rather adhere. This *adhesion model* is just the three-dimensional Burgers equation (1.1), taken in the limit of vanishing viscosity. Numerical experiments indicate that the adhesion model reproduces quite well the early skeleton of large-scale structures in N-body numerical simulations (see, for example, Figs. 6a and 6b of Ref. [11]). Since dark matter is essentially collisionless, it is not clear at the moment what is the physics behind this agreement which seems to require some viscosity-generating mechanism to prevent – or dramatically slow down – particle crossing. Furthermore, the adhesion model cannot cope with many important aspects of gravitational dynamics. For example, in N-body simulations, one frequently observes the collapse of

a filament into an isolated node (cluster). As we shall see, there is nothing of this sort in Burgers dynamics.

1.2 The Burgers equation in condensed matter and statistical physics

The Burgers equation arises in a number of condensed matter and statistical physics problems and even in non-physics problems such as vehicular traffic (for review see Ref. [12]) A frequently studied problem is the Kardar–Parisi–Zhang or KPZ equation [13] (see also Ref. [14])

$$\partial_t \psi = \frac{1}{2} |\nabla \psi|^2 + \nu \nabla^2 \psi + F, \tag{1.2}$$

which appears in studying the motion of an interface under deposition. Here, ψ is the vertical displacement of the interface as a function of $d-1$ horizontal coordinates and of the time. It is immediately checked, by taking the horizontal gradient of (1.2), that one obtains the Burgers equation (1.1) with an additional forcing term $\mathbf{f} = -\nabla F$. Burgers equation also arises in studying directed polymers (see, *e.g.* [15, 16]), but with the time variable now interpreted as a space variable in the direction of main extension of the polymers. On all these problems there is considerable literature which it is not our purpose to review here.

1.3 The Burgers equation as testing ground for Navier–Stokes

The Burgers equation, because of its known solutions, is frequently used for testing numerical schemes, particularly those intended for compressible flow (many of the Google hits are of this kind). If one is mostly interested in turbulence, as is the case for participants of the present School, Burgers equation turns out to be quite useful for testing – and mostly discarding – certain types of theories of turbulence. Indeed, there have been many attempts to tackle the problem of the statistical theory of turbulence by adapting to it tools borrowed from field theory (for reviews, see [17–20]). Such methods had little impact on the field until recently when they have permitted a real breakthrough in understanding the mechanism for intermittency and anomalous scaling (see, *e.g.* the lectures by Falkovich *et al.* in the same volume). In the past such field-theoretic methods have frequently involved formal expansions in powers of the nonlinearity, with Feynman graphs used for the bookkeeping of all the terms generated after averaging over Gaussian initial conditions and/or random forces. Since the Burgers equation has the same type of nonlinearity as the Navier–Stokes equation such methods are typically also applicable to the Burgers equation. Hence it is possible to find what they predict for the latter and to compare the results with those obtained by more reliable methods. From this point of

view, that is of using the Burgers equation as testing ground, it is desirable to know the answers to questions similar to those generally asked for Navier–Stokes turbulence. For example, what are the scaling properties of structure functions; what are the probability distribution functions (pdf) of velocity increments and velocity gradients? Such questions will be at the center of these lectures. Whenever possible we shall comment on the corresponding Navier–Stoke issues. The emphasis will be exclusively on what happens in the real space-time domain in the limit of vanishing viscosity, which is of course not the same as naively putting the viscosity equal to zero. A number of interesting questions, requiring a finite viscosity, such as the pole decomposition [21, 22] will thus be left out.

2 Basic tools

In this section we introduce various analytical, geometrical and numerical tools which are useful for constructing solutions to the decaying (unforced) Burgers equation (1.1). Mostly, we shall deal with the deterministic equation, while making occasional comments on consequences for burgulence.

2.1 The Hopf–Cole transformation and the maximum representation

If in (1.2) with $F = 0$ we set $\psi = 2\nu \ln \theta$ we obtain the d-dimensional heat equation [1, 2]

$$\partial_t \theta = \nu \nabla^2 \theta, \tag{2.1}$$

which can be solved explicitly if there are no boundaries. One thus obtains

$$\psi(\mathbf{r}, t) = 2\nu \ln \left\{ \frac{1}{(4\pi\nu t)^{d/2}} \int_{\mathbb{R}^d} \exp\left[\frac{1}{2\nu} \left(\psi_0(\mathbf{a}) - \frac{|\mathbf{r}-\mathbf{a}|^2}{2t} \right) \right] \mathrm{d}^d a \right\}, \tag{2.2}$$

where $\psi_0(\mathbf{a})$ is the initial potential. The limit of vanishing viscosity ($\nu \to 0$), obtained by steepest descent, has the following "maximum representation"

$$\psi(\mathbf{r}, t) = \max_{\mathbf{a}} \left(\psi_0(\mathbf{a}) - \frac{|\mathbf{r}-\mathbf{a}|^2}{2t} \right). \tag{2.3}$$

Note that the operation of taking a maximum is global in nature, whereas the viscous Burgers equation is a local partial differential equation. If $\psi_0(\mathbf{a})$ is differentiable (*i.e.* the initial velocity $\mathbf{u}_0(\mathbf{a})$ exists as an ordinary function rather than a distribution), the maximum in (2.3) will be achieved at one or several points $\mathbf{a}$ where the gradient of the r.h.s. vanishes, that is, where

$$\mathbf{r} = \mathbf{a} + t\mathbf{v}_0(\mathbf{a}). \tag{2.4}$$

In other words, $\mathbf{r}$ is the position at time t of the fluid particle starting at $\mathbf{a}$ and retaining its initial velocity $\mathbf{v}_0(\mathbf{a})$. Hence, we can interpret $\mathbf{a}$ and

r as being, respectively, Lagrangian and Eulerian coordinates. Along this Lagrangian trajectory, the velocity being conserved, we have

$$\mathbf{v}(\mathbf{r},t) = \mathbf{v}_0(\mathbf{a}). \tag{2.5}$$

The map $\mathbf{a} \mapsto \mathbf{r}$ defined by (2.4) is called the naive Lagrangian map. It is not necessarily invertible: if there are several Lagrangian locations satisfying (2.4) for a given $\mathbf{r}$ the only acceptable one is that which maximizes the argument on the r.h.s. of (2.3). As long as the Jacobian of the naive Lagrangian map (2.4)

$$J(\mathbf{a},t) = \det\left(\delta_{ij} - t\frac{\partial^2\psi_0}{\partial a_i \partial a_j}\right) \tag{2.6}$$

does not vanish the map is guaranteed to be invertible and the solution of the Burgers equation cannot have a singularity. For sufficiently smooth initial data with bounded second derivatives of ψ_0 the first singularity appears at

$$t_\star = \frac{1}{\max_{\mathbf{a}}\left[\lambda(\mathbf{a})\right]}, \tag{2.7}$$

where $\lambda(\mathbf{a})$ is the largest eigenvalue of the Hessian matrix $\partial^2\psi_0/\partial a_i \partial a_j$.

In one dimension, we denote the velocity by u. Now, the time $t_\star$ is the inverse of the absolute value of the most negative initial velocity derivative $\mathrm{d}u_0(a)/\mathrm{d}a$. It is the first time at which the characteristics $x = a + tu_0(a)$ of the hyperbolic inviscid Burgers equation are crossing (Fig. 3). The first

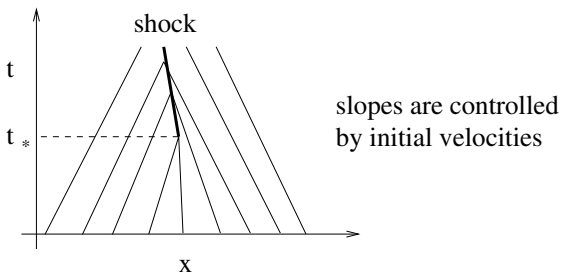

Fig. 3. Characteristics for the unforced one-dimensional Burgers equation in the (x,t) plane.

singularity in one or more dimension, is known as a "preshock" [23] and plays an important role in the theory of pdf for velocity gradients and densities (Sects. 6 and 7).

Note that, for Gaussian random initial conditions, $t_\star$ is itself random and can become arbitrarily small with very small but nonvanishing probability.

As a consequence, most averaged quantities (*e.g.* the two-point correlation function) will have an essential singularity at $t = 0$. Note also that the distribution of eigenvalues of the Hessian matrix extends to infinite values in any finite dimension d, but becomes compactly supported (on a semi-circle) when dividing the eigenvalues by $\sqrt{d}$ and letting $d \to \infty$. This is indeed a consequence of the properties of large random symmetric matrices, called Wigner matrices (see, *e.g.*, Ref. [25]).

2.2 Shocks in one dimension

After the time $t_\star$ the Lagrangian map (2.4) ceases to be invertible. More precisely, for a given Eulerian position $\mathbf{r}$ there is more than one Lagrangian position $\mathbf{a}$ satisfying (2.4). This implies the presence of shocks in the Eulerian velocity field. In this subsection we consider the one-dimensional case and give various geometrical constructions of the solution (including shocks).

First, let us define in the (x, ψ)-plane the Lagrangian manifold (a curve in one dimension)

$$x \equiv a + tu_0(a) \tag{2.8}$$

$$\psi \equiv \psi_0(a) - \frac{t}{2}u_0^2(a), \tag{2.9}$$

where the second line is just the r.h.s. of (2.3) without the maximum, evaluated at the (naive) Eulerian position $a + tu_0(a)$. Figure 4 (upper) shows this Lagrangian manifold after the time $t_\star$. Hence, above some Eulerian locations x there is more than one branch and cusps are present at Eulerian locations such that the number of branches changes. Clearly, the correct Eulerian potential is obtained by taking the maximum, *i.e.* always the highest branch. Note that this potential will have one or several points with discontinuous slope, the right derivative being always greater than the left one. Hence the velocity, which is the negative space derivative of the potential (shown in the lower part of Fig. 4) will have discontinuities at shock locations with $u_- > u_+$. It is also possible to directly construct the velocity starting from the Lagrangian manifold in the (x, u)-plane

$$x \equiv a + tu_0(a) \tag{2.10}$$

$$u \equiv u_0(a). \tag{2.11}$$

If there is a single shock present, it follows obviously that its position is determined by a Maxwell rule: the hashed loops shown in Figure 4 (lower part) right and left of the shock should have equal areas. A Maxwell rule construction can become very cumbersome if there are several shocks present.

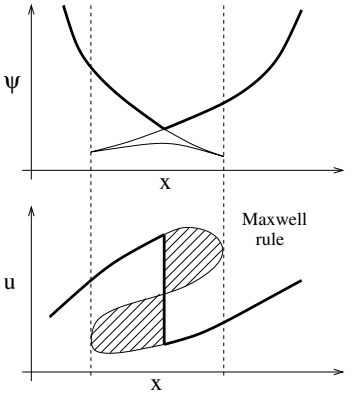

Fig. 4. Lagrangian manifolds for the potential in the (x, ψ)-plane (upper) and the velocity in the (x, u)-plane (lower). The heavy lines correspond to the correct Eulerian solutions. The vertical dashed lines delineate the multivalued region.

Another geometrical construction uses the *Lagrangian potential*

$$\varphi(a,t) \equiv t\psi_0(a) - \frac{a^2}{2}, \tag{2.12}$$

whose negative gradient is obviously the naive Lagrangian map. We can rewrite (2.3) as

$$t\psi(x,t) + \frac{x^2}{2} = \max_a \left[\varphi(a,t) + ax\right], \tag{2.13}$$

which represents the potential as, basically, a Legendre transform of the Lagrangian potential. (Note that the Legendre transformation is also used in the theory of multifractals.) The r.h.s. of (2.13) is equivalent to finding the largest algebraic vertical distance between the graph of the Lagrangian potential and the line of slope $-x$ through the origin. If the graph is convex (second derivative negative everywhere), the maximum is attained at the unique point where the derivative has the value $-x$. Otherwise, it suffices to replace the graph of φ by its convex hull φ_c, that is the intersection of all half-planes containing the graph. This is illustrated in Figure 5, which shows both regular points (Lagrangian points which have not fallen into a shock) and one shock interval, situated below the segment which is part of the convex hull. Again, it is possible to work directly with the (negative) derivative of the Lagrangian potential, namely, the naive Lagrangian map. The convex hull construction becomes then a Maxwell rule as shown in Figure 6. From this one can easily show that the speed of a shock is the half-sum of the velocities immediately to the right and to the left.

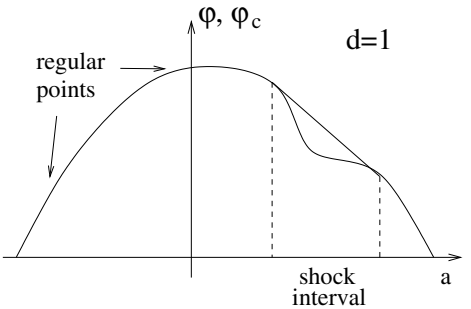

Fig. 5. Convex hull construction in terms of the Lagrangian potential.

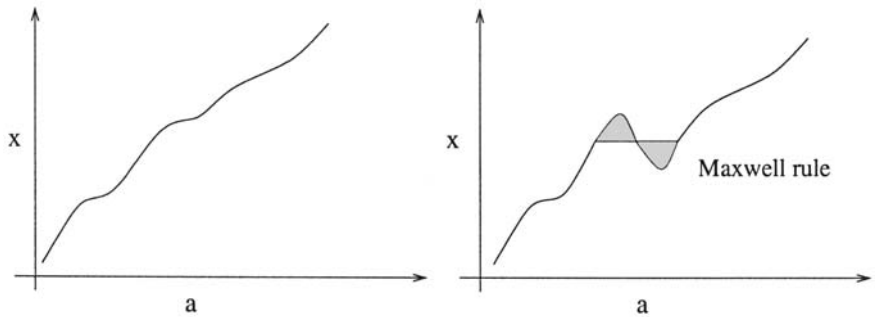

Fig. 6. Naive Lagrangian map before (left) and after (right) appearance of a shock. The correct Lagrangian map is obtained by a Maxwell rule.

Finally, the maximum formula (2.3) yields directly a "parabola construction", illustrated in Figure 7: a parabola with apex at x and radius of curvature proportional to t is moved down until it touches the initial potential $\psi_0(a)$ at the Lagrangian location associated to x (or at two such locations if there is a shock). Which of the five geometrical methods given is more convenient depends on the application considered. The parabola construction is best for understanding evolution in time (*cf.* Sect. 4). It may be used, for example, to show that the long-time Eulerian solution has a sawtooth structure with shocks separated by ramps of slope $1/t$ (see Fig. 14). The ramps are associated to high local maxima in the potential ψ_0.

With random and homogeneous initial conditions there will be shocks (discontinuities) at random Eulerian locations which do not cluster (unless we use non-smooth initial conditions as in Sect. 5). From this it is easily

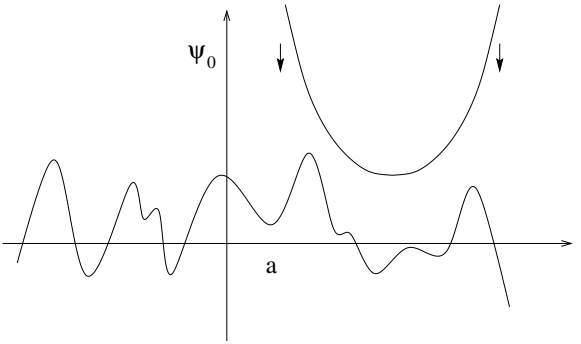

Fig. 7. Parabola construction of the solution.

inferred that, for $p > 0$, the structure functions

$$S_{\rm p}(\Delta x, t) \equiv \langle |u(x + \Delta x, t) - u(x, t)|^p \rangle \tag{2.14}$$

behave, for small Δx, as

$$S_{\rm p}(\Delta x, t) \sim C_{\rm p} |\Delta x|^p + C'_{\rm p} |\Delta x|, \tag{2.15}$$

where the first term comes from regular (smooth) parts of the Eulerian velocity, while the second comes from the $O(|\Delta x|)$ probability to have a shock somewhere in an interval of Eulerian length $|\Delta x|$. For $0 < p < 1$ the first term dominates as $\Delta x \to 0$, while, for $p > 1$, it is the second. Hence, $S_{\rm p} \sim |\Delta x|^{\zeta_{\rm p}}$, with the exponents $\zeta_{\rm p}$ as shown in Figure 8. There are also higher-order corrections to the simple scaling law given in (2.15) which cannot be obtained by such simple arguments [30]. Note that a second-order structure functions with a behavior $\propto |\Delta x|$ at small distances implies an energy spectrum $E(k) \propto k^{-2}$ as $k \to \infty$.

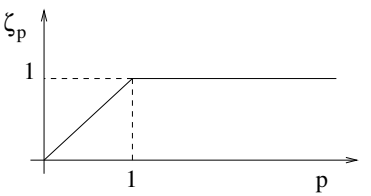

Fig. 8. Exponent of the structure function of order p. Note the "phase transition" at $p = 1$.

The "phase transition" at $p = 1$ seen in Figure 8 is due to the isolated character of the dissipative structures (the shocks), a feature not present in incompressible three-dimensional Navier–Stokes turbulence.

2.3 Convex hull construction in more than one dimension

Some of the methods used for the one-dimensional case are readily extended to dimensions $d > 1$, for example the construction from the Lagrangian manifold in the $(d+1)$ dimensional space $(\mathbf{x}, \psi)$. In Section 7 we shall use the multidimensional generalization of the convex hull construction, which we now briefly outline. We define the Lagrangian potential

$$\varphi(\mathbf{a}, t) \equiv -\frac{|\mathbf{a}|^2}{2} + t\psi_0(\mathbf{a}). \tag{2.16}$$

and find, from (2.3), that

$$t\psi(\mathbf{r}, t) + \frac{|\mathbf{r}|^2}{2} = \max_{\mathbf{a}} \left[\varphi(\mathbf{a}, t) + \mathbf{r} \cdot \mathbf{a}\right]. \tag{2.17}$$

As before, this involves a (multidimensional) Legendre transformation which leads us to the construction of the convex hull in a $(d+1)$ dimensional space of the graph of the Lagrangian potential. In more than one dimension, singularities of convex hulls are considerably more involved. As a consequence, the equivalent of shocks are discontinuities across $(d-1)$ manifolds, but there are many other singularities of higher codimension (the codimension is d minus the dimension of the object).

In two dimensions the convex hull consists generically of four kinds of objects: (i) parts of the original graph, (ii) pieces of ruled surfaces, (iii) "kurtoparabolic points", to which we shall come back, and (iv) triangles (see Fig. 9). The associated Eulerian objects are, respectively, (i) regular points, (ii) shock lines, (iii) end points of shocks and (iv) shock nodes. Likewise, in three dimensions we have two-dimensional shock surfaces meeting in triples at shock lines, meeting in quadruples at shock nodes. (Nodes are always connected to shock lines and never isolated.) Note that the Eulerian part of Figure 9 looks just like a thermodynamic phase diagram, with the three shock lines playing the role of the liquid-gas, liquid-solid and solid-gas transition lines, the node playing the role of the triple point and the end point the role of the critical point. This is not accidental. In thermodynamics, equilibrium states are obtained by minimizing the Gibbs potential. This is equivalent to taking a Legendre transform of the internal energy in which the pressure and the temperature play the role of the Eulerian coordinates [26]. This analogy holds also in higher dimensions: the classification of "Legendrian singularities" can be used both for studying the Burgers equation [27] and for studying multi-variable phase transitions [28].

A more complete description of singularities is obtained by considering the metamorphoses of singularities as time elapses. A complete classification in two and three dimensions may be found in the appendix (supplement 2) by Arnold *et al.* of reference [3].

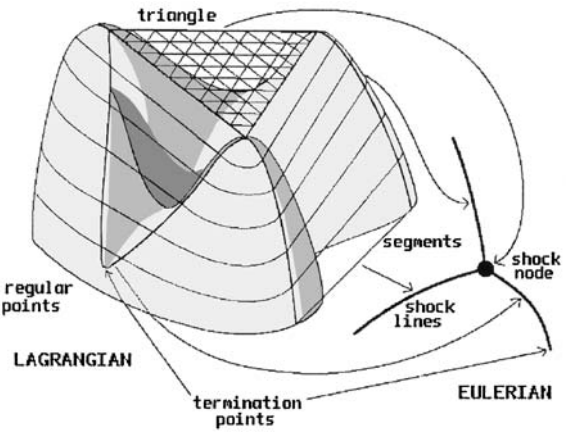

Fig. 9. Construction of the convex hull for a two-dimensional Lagrangian potential and associated Eulerian picture (figure adapted from Ref. [7]).

For random initial conditions the structure functions scale the same way as in one dimension. For example, the probability of having a $(d-1)$-dimensional shock intercepting an Eulerian segment of small length r is $O(r)$. The higher codimension structures give only subdominant corrections.

2.4 Remarks on numerical methods

Here, we give just some indications on how the (decaying) Burgers equation can be solved numerically. (For more details, see [7, 29, 30] or any textbook on numerical methods for nonlinear hyperbolic equations; for the case with forcing, see [15, 30] and references therein.) First, one can of course, solve the Burgers equation with viscosity. This should be avoided unless one is interested in what happens at dissipative scales (*e.g.*, inside shocks). For the inviscid limit and only in the decaying case it is possible to construct the solution at time t directly from the initial condition without recourse to any time marching. One way is to directly use the maximum representation (2.3), assuming that Lagrangian and Eulerian locations have been discretized on the same grid. Then, for a given Eulerian $\mathbf{r}$ one searches the Lagrangian $\mathbf{a}$ which maximizes the r.h.s. If there are N grid points, this seems to require $O(N^2)$ operations, but it can actually be done in $O(N \log_2 N)$ operations [7, 29]. Such a strategy must be combined with suitable interpolations to increase accuracy and avoid getting complete garbage for derivatives [30]. In one dimension one can also use Lagrangian strategies with particle and/or shock tracking. To be consistent with the

inviscid limit, the particles must stick upon collisions. for sufficiently smooth initial data, it may be possible to construct the solution from the Lagrangian manifold (2.8, 2.9) or its multidimensional generalization, by just searching the maximum, for a given $\mathbf{x}$, of the finitely many branches present.

3 The Fourier–Lagrange representation and artefacts

In this section we show that formal manipulations of the inviscid Burgers equation with random initial conditions, even though they include apparently terms of all orders, can nevertheless lead to completely incorrect results, *e.g.* for the energy spectrum. This section is entirely based on work by Fournier and Frisch [23]. The theory is given in one dimension but similar results can be established in higher dimensions.

In one dimension, it follows from (2.10, 2.11), that the Eulerian solution to the initial value problem for the decaying Burgers has the following implicit representation:

$$\begin{aligned} u(x,t) &= u_0(a) \\ x &= a + tu_0(a). \end{aligned} \tag{3.1}$$

This becomes explicit if, instead of working with $u(x,t)$, we use its spatial Fourier transform (2π-periodicity is assumed for convenience)

$$\hat{u}(k,t) \equiv \frac{1}{2\pi}\int_0^{2\pi} \mathrm{e}^{-ikx} u(x,t)\,\mathrm{d}x \tag{3.2}$$

and make the change of variables $x \mapsto a$, to obtain

$$\hat{u}(k,t) = \frac{1}{2\pi}\int_0^{2\pi} \mathrm{e}^{-ikx(a,t)}\, u_0(a)\frac{\partial x}{\partial a}\,\mathrm{d}a, \quad x(a,t) \equiv a + tu_0(a). \tag{3.3}$$

Equation (3.3) is called the *Fourier–Lagrangian* representation. A first integration by parts yields

$$\hat{u}(k,t) = \frac{1}{2\pi}\frac{1}{ik}\int_0^{2\pi} \mathrm{e}^{-ik(a+tu_0(a))}\, u_0'(a)\,\mathrm{d}a. \tag{3.4}$$

A second integration by parts leads then to

$$\hat{u}(k,t) = \frac{1}{2\pi}\frac{1}{ikt}\int_0^{2\pi} \mathrm{e}^{-ik(a+tu_0(a))}\,\mathrm{d}a, \quad k \neq 0. \tag{3.5}$$

If we now take random homogeneous Gaussian initial conditions, we can easily calculate moments of $\hat{u}(k,t)$ because they just involve averages of

exponentials having the Gaussian initial velocity in their arguments. For example, the energy spectrum, related to the correlation function by

$$\langle \hat{u}(k,t)\hat{u}(k',t)\rangle = E(k,t)\delta_{k,k'}, \tag{3.6}$$

where $\delta_{k,k'}$ is a Kronecker delta, has the following expression

$$E(k,t) = \frac{1}{2\pi}\frac{1}{k^2t^2}\int_0^{2\pi} \mathrm{e}^{-ikh}\mathrm{e}^{-\frac{1}{2}k^2t^2S_2(h,0)}\,\mathrm{d}h, \tag{3.7}$$

where $S_2(h,0) \equiv \left\langle [u_0(h)-u_0(0)]^2 \right\rangle$ is the second-order structure function of the initial velocity field. If the latter is smooth, as we shall assume, we have $S_2(h,0) \propto h^2$ for $h \to 0$. It then follows by a simple Laplace-type asymptotic expansion of (3.7) that

$$E(k,t) \propto k^{-3} \quad \text{when} \quad k \to \infty. \tag{3.8}$$

This is obviously the wrong answer: for Gaussian initial conditions there will be shocks with a non-vanishing probability for any $t > 0$. Their signature is a k^{-2} law in the energy spectrum at high wavenumbers, as shown in Section 2.2.

What went wrong? After the appearance of the first shock the Lagrangian map $a \mapsto x$ is not monotonic and the change of variable from (3.2) to (3.3) is valid only outside of the Lagrangian shock interval. Hence, in (3.3) we should excise this interval from the domain of integration. If we do not remove it, we are actually calculating the Fourier transform of a function obtained by superposing the threee branches shown in Figure 10 with a plus sign for the two direct branches and a minus sign for the retrograde branch (the sign comes from the lack of an absolute value on the Jacobian $\partial x/\partial a$ in (3.3)). Obviously, this superposition has two square-root cusps as shown in Figure 10. This produces $k^{-3/2}$ tails in the Fourier transform and, hence, explains the spurious k^{-3} energy spectrum. Note also that this superposition of three branches is not a solution to the Burgers equation, the latter being nonlinear. This phenomenon is not related to the well known non-uniqueness of the solution to the Burgers equation with zero viscosity without proper additional conditions [24].

The problem is actually worse than suggested so far. It is easily shown that if the the initial velocity is deterministic and smooth, the function of the time defined by (3.3), for *fixed* wavenumber k, is entire, that is, its Taylor series around $t = 0$ has an infinite radius of convergence. There is no way to see the time $t_\star$ of the first preshock from this function. A preshock is indeed an "ultraviolet" singularity which is not seen in the temporal behavior of a single spatial Fourier component. This result has an important

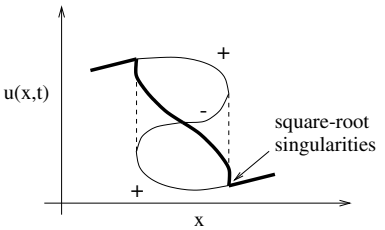

Fig. 10. Spurious solution of Burgers equation when three branches of a multivalued solution are combined into one.

consequence for the case of random Gaussian initial conditions. Suppose we simply ignore the viscosity in the Burgers equation and expand the solution to all orders in a temporal Taylor series around $t = 0$ and then calculate various correlation functions and use Feynman graphs for bookkeeping of all the terms generated from averaging. We then find that the whole set can be resummed exactly and gives a spectrum with a k^{-3} tail. Of course, the origin of the "resummation miracle" is the Fourier–Lagrangian representation.

4 The law of energy decay

An important issue in burgulence and turbulence is that of the law of decay at long times when the viscosity is very small. Before turning to the Burgers equation let us recall a few things about the Navier–Stokes case. It is generally believed that high-Reynolds number turbulence has universal and non-trivial small-scale properties. In contrast, large scales, important for practical applications such as transport of heat or pollutants, are believed to be non-universal. This is however so only for the toy model of turbulence maintained by prescribed large-scale random forces. Very high-Reynolds number turbulence, decaying away from its production source, and far from boundaries can relax under its internal nonlinear dynamics to a (self-similarly evolving) state with universal and non-trivial statistical properties *at all scales*. Kármán and Howarth [31], investigating the decay of high-Reynolds number, homogeneous isotropic three-dimensional turbulence, proposed a self-preservation (self-similarity) ansatz for the spatial correlation function of the velocity: the correlation function keeps a fixed functional shape; the integral scale $L(t)$, characteristic of the energy-carrying eddies, grows in time and the mean kinetic energy $E(t) = u^2(t)$ decays, both following power laws; there are two exponents which can be related by the condition that the energy dissipation per unit mass $|\dot{E}(t)|$ should be proportional to u^3/L. But *an additional relation* is needed to actually determine the exponents. The invariance in time of the energy

spectrum at low wavenumbers, known as the "permanence of large eddies" [19, 20, 34] can be used to derive the law of self-similar decay when the initial spectrum $E_0(k) \propto k^n$ at small wavenumbers k, with n below a critical value equal to 3 or 4, the actual value being disputed because of the "Gurbatov phenomenon" (see the end of this section). One then obtains a law of decay $E(t) \propto t^{-2(n+1)/(3+n)}$. (Kolmogorov [32] proposed a law of energy decay $u^2(t) \propto t^{-10/7}$, which corresponds to $n = 4$ and used in its derivation the so-called "Loitsyansky invariant", a quantity actually not conserved, as shown by Proudman and Reid [33].) When the initial energy spectrum at low wavenumbers goes to zero too quickly, the permanence of large eddies cannot be used, because the energy gets backscattered to low wavenumbers by nonlinear interactions. For Navier–Stokes turbulence the true law of decay is then known only within the framework of closure theories (see, *e.g.* [20]).

For one-dimensional burgulence, many of these questions are completely settled. First, we observe that the problem of decay is quite simple if a finite spatial periodicity is assumed. Indeed, eventually, all the shocks produced will merge into a single shock per period, as shown in Figure 11. The position of the shock is random and the two ramps have slope $1/t$, as is easily shown using the parabola construction of Section 2.2. Hence, the law of decay is simply $E(t) \propto t^{-2}$. Nontrivial laws of decay are obtained

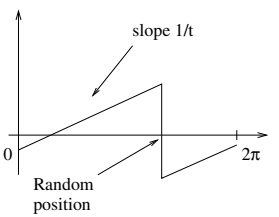

Fig. 11. Snapshot of solution of decaying burgulence at long times when spatial periodicity is assumed.

if the burgulence is homogeneous in an unbounded domain and has the "mixing" property (which means, roughly, that correlations are decreasing with separation). The number of shocks is then typically infinite but their density per unit length is finite and decreases in time because shocks are constantly merging. The $E(t) \propto t^{-2(n+1)/(3+n)}$ law mentioned above can be derived for burgulence from the permanence of large eddies when $n \leq 1$ [34]. For $n = 0$, this $t^{-2/3}$ law was actually derived by Burgers himself [35].

The hardest problem is again when permanence of large eddies does not determine the outcome, namely for $n > 1$. This problem was solved by Kida [36] (see also Refs. [3, 23, 34]).

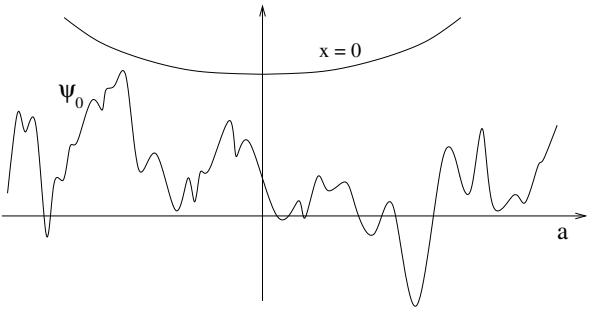

Fig. 12. An initial potential which is everywhere below the parabola $a^2/(2t)+\psi$. The probability of such events gives the cumulative probability to have a potential at time t less than ψ.

We now give some key ideas regarding the derivation of Kida's law of energy decay. We assume Gaussian, homogeneous smooth initial conditions, such that the potential is homogeneous. Since a homogeneous function is not, in general, the derivative of another homogeneous function, we assume that the initial energy spectrum

$$E_0(k) \propto k^n, \quad n > 1; \quad k \to 0. \tag{4.1}$$

This condition implies that the mean square initial potential $\int k^{-2} E_0(k)\,\mathrm{d}k$ has no infrared (small-k) divergence (the absence of an ultraviolet divergence is guaranteed by the assumed smoothness).

A very useful property of decaying burgulence, with no known counterpart for Navier–Stokes turbulence, is the relation

$$E(t) = \frac{\partial}{\partial t} \langle \psi \rangle \,, \tag{4.2}$$

which follows by taking the mean of (1.2) in the absence of a driving force. Hence, the law of energy decay can be obtained from the law for the mean potential. The latter can be derived from the cumulative probability of the potential which, by homogeneity, does not depend on the position. By (2.3), its expression at $x = 0$ is

$$\mathrm{Prob}\,\{\mathrm{Potential} < \psi\} = \mathrm{Prob}\left\{\forall a, \;\; \psi_0(a) < \frac{a^2}{2t} + \psi\right\}. \tag{4.3}$$

Expressed in words, we want to find the probability that the initial potential does not cross the parabola $a^2/(2t)+\psi$ (see Fig. 12). Since, at long times t, the relevant ψ is going to be large, the problem becomes that of not crossing a parabola with small curvature and very high apex. Such crossings, more

precisely the upcrossings, are spatially quite rare. As a consequence of the mixing property, for long t, they form a Poisson process [37] for which

$$\text{Prob}\,\{\text{no crossing}\} \simeq \mathrm{e}^{-\langle N(t)\rangle}, \tag{4.4}$$

where $\langle N(t)\rangle$ is the mean number of upcrossings. By the Rice formula (a consequence of the identity $\delta(\lambda x) = (1/|\lambda|)\delta(x)$,

$$\langle N(t)\rangle = \left\langle \int_{-\infty}^{+\infty} \mathrm{d}a\; \delta\left(m(a) - \psi\right) \frac{\mathrm{d}m}{\mathrm{d}a}\; H\left(\frac{\mathrm{d}m}{\mathrm{d}a}\right) \right\rangle, \tag{4.5}$$

where H is the Heaviside function and

$$m(a) \equiv \psi_0(a) - \frac{a^2}{2t}\cdot \tag{4.6}$$

Since $\psi_0(a)$ is Gaussian, the r.h.s. of (4.5) can be easily expressed in terms of integrals over the probability densities of $\psi_0(a)$ and of $\mathrm{d}\psi_0(a)/\mathrm{d}a$ (as a consequence of homogeneity these variables are uncorrelated and, hence, independent). The resulting integral can then be expanded by Laplace's method for large t, yielding

$$\langle N(t)\rangle \sim t^{1/2}\psi^{-1/2}\mathrm{e}^{-\psi^2}, \quad t \to \infty. \tag{4.7}$$

When this expression is used in (4.4) and the result is differentiated with respect to ψ to obtain the pdf of $p(\psi)$, the latter is found to be concentrated around $\psi_\star = (\ln t)^{1/2}$ (see Fig. 13). It then follows that, at large times, we

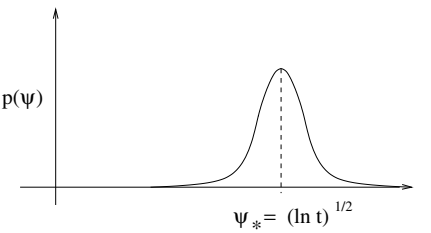

Fig. 13. A sketch of the pdf of the potential at long times.

have Kida's log-corrected $1/t$ law for the energy decay

$$\langle\psi\rangle \sim (\ln t)^{1/2}, \quad E(t) \sim \frac{1}{t(\ln t)^{1/2}}, \quad L(t) \sim \frac{t^{1/4}}{(\ln t)^{1/4}}\cdot \tag{4.8}$$

The Eulerian solution, at long times, has the ramp structure shown in Figure 14 with shocks of typical strength $u(t) = E^{1/2}(t)$, separated typically by a distance $L(t)$. The growth in time of $L(t)$ takes place because

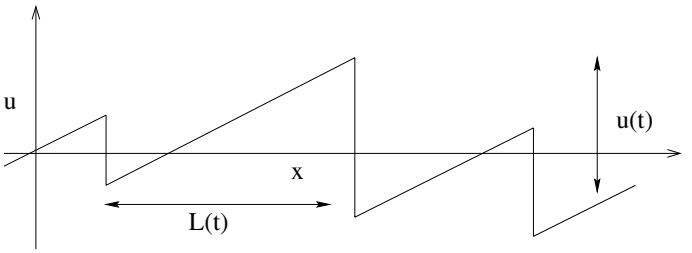

Fig. 14. The Eulerian solution at long times t. The ramps have slope $1/t$. In time-independent scales, the figure would be stretched horizontally and squeezed vertically by a factor proportional to t.

correlated particles, which initially cannot be much apart, may propagate to far-apart locations at long times.

The fact that Kida's law is valid for any $n > 1$, and not just for $n \geq 2$ as thought originally, gives rise to an interesting phenomenon now known as the "Gurbatov effect": if $1 < n < 2$ the long-time evolution of the energy spectrum cannot be globally self-similar. Indeed, the permanence of large eddies, which is valid for any $n < 2$ dictates that the spectrum should preserve exactly its initial $C_n k^n$ behavior at small wavenumbers k, with a constant-in-time C_n. Global self-similarity would then imply a $t^{-2(n+1)/(3+n)}$ law for the energy decay, which would contradict Kida's law. Actually, as shown in [34], for $1 < n < 2$ there are two characteristic wavenumbers with different time dependences, the integral wavenumber $k_{\mathrm{L}}(t) \sim (L(t))^{-1}$ and a switching wavenumber $k_{\mathrm{s}}(t) \ll k_{\mathrm{L}}(t)$ below which holds the permanence of large eddies. It was shown that the same phenomenon is also present in the decay of a passive scalar [38]. Whether or not a similar phenomenon is present in three-dimensional Navier–Stokes incompressible turbulence or closure models thereto is a controversial matter [39, 40].

For decaying burgulence, if we leave aside the Gurbatov phenomenon which does not affect energy-carrying scales, the following may be shown. If we rescale distances by a factor $L(t)$ and velocities amplitudes by a factor $u(t) = E^{1/2}(t)$ and then let $t \to \infty$, the spatial (single-time) statistical properties of the whole random velocity field become time-independent. In other words, there is a self-similar evolution at long times. Hence, dimensionless ratios such as the velocity flatness

$$F(t) \equiv \frac{\left\langle u^4 \right\rangle (t)}{\left[\left\langle u^2 \right\rangle (t) \right]^2} \tag{4.9}$$

have a finite limit as $t \to \infty$. A similar property holds for the the decay of passive scalars [41]. We do not know if this property holds also

for Navier–Stokes incompressible turbulence or if, say, the velocity flatness grows without bound at long times.

5 One-dimensional case with Brownian initial velocity

Burgers equation, when the initial velocity is Gaussian with a power-law spectrum $\propto k^{-n}$, is what cosmologists call *scale-free* initial conditions (see Refs. [8,9]). Here, we consider the one-dimensional case with Brownian motion (in the space variable) as initial velocity, corresponding to $n = 2$. The general case, including higher dimensions, is discussed in [7] (an example of a 2-D simulation with scale-free initial data is shown in Fig. 2).

Brownian motion is continuous but not differentiable (see Fig. 15); hence, shocks appear after arbitrarily short times and are actually *dense* (see Fig. 16). Numerically supported conjectures made in [6], have led to a proof by Sinai [42] of the following result: in Lagrangian coordinates, the regular points, that is fluid particles which have not yet fallen into shocks, form a fractal set of Hausdorff dimension 1/2. This implies that there is a Devil's staircase of dimension 1/2 in the Lagrangian map (see Fig. 18). Note that when the initial velocity is Brownian, the Lagrangian potential has a second space derivative which is delta-correlated in space; this can be approximately pictured as a situation where the Lagrangian potential has very strong oscillations in curvature. Hence, it is not surprising that very few points of its graph can belong to its convex hull (see Fig. 17).

We will now give some highlights of Sinai's proof of this result. For this problem, it turns out that the Hausdorff dimension of the regular points (determined in Ref. [42]) is also equal to its box-counting dimension, which is easier to determine. One obtains the latter by finding the probability that

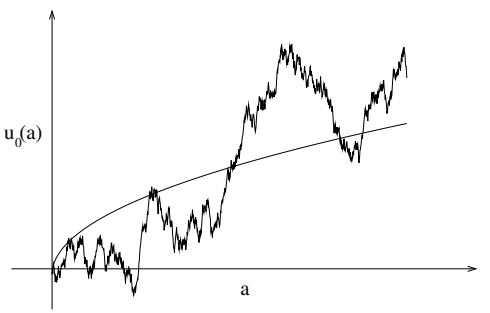

Fig. 15. A realization of the Brownian motion curve. The parabola shows the root-mean-square velocity $\propto a^{1/2}$.

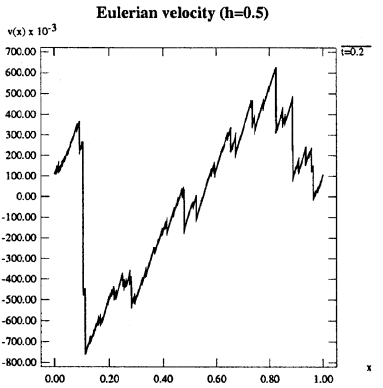

Fig. 16. Snapshot of the velocity resulting from Brownian initial data. Notice the dense proliferation of shocks (from Ref. [7]).

Fig. 17. Sketch of the Lagrangian potential together with its convex hull (from Ref. [7]).

a small Lagrangian interval of length ℓ contains at least one regular point which belongs simultaneously to the graph of the Lagrangian potential φ and to its convex hull. In other words, one looks for points, such as R, with the property that the graph of φ lies below its tangent at R (see Fig. 19). Sinai does this by the box construction with the following constraints on the graph:

Left: the graph of the potential should be below the half line Γ_-;

Right: the graph of the potential should be below the half line Γ_+;

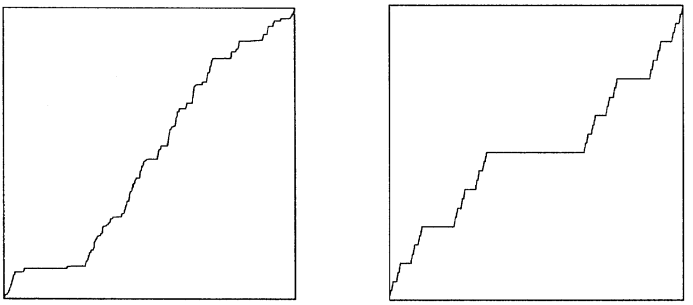

Fig. 18. Left: the Lagrangian map looks like a devil's staircase. Right: standard devil's staircase over the triadic Cantor set, which is constant almost everywhere, except on a fractal (from Ref. [7]).

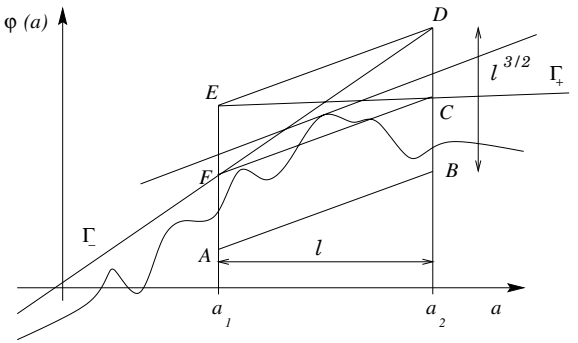

Fig. 19. The box construction used to find a regular point R (point of tangency with the graph entirely on one side of the tangent) within a Lagrangian interval of length ℓ (from Refs. [7, 42]).

$$\textit{Box}: \begin{cases} 1\text{: enter } (AF) \text{ with a slope larger than that of } \Gamma_- \text{ by } O(\ell^{1/2}) \\ 2\text{: exit } (CB) \text{ with a slope less than that of } \Gamma_+ \text{ by } O(\ell^{1/2}) \\ 3\text{: cross } (FC) \text{ and stay below } (ED). \end{cases}$$

It is obvious that such conditions ensure the existence of at least one regular point. (Move (ED) down parallel to itself until it touches the graph.) Note that A and the slope of (AB) are prescribed. Hence, one is calculating conditional probabilities; but it may be shown that the conditioning is not affecting the scaling dependence on ℓ.

As the Brownian motion $u_0(a)$ is a *Markov process*, the constraints *Left*, *Box* and *Right* are independent and hence,

$$\begin{aligned} P^{\text{reg.}}(\ell) &\equiv \text{Prob}\{\text{regular point in interval of length } \ell\} \\ &= \text{Prob}\{\textit{Left}\} \times \text{Prob}\{\textit{Box}\} \times \text{Prob}\{\textit{Right}\} \cdot \end{aligned} \tag{5.1}$$

The scales of the box were chosen so that $\text{Prob}\{\textit{Box}\}$ is independent of ℓ:

$$\text{Prob}\{\textit{Box}\} \sim \ell^0. \tag{5.2}$$

Indeed, Brownian motion and its integral have scaling exponent $1/2$ and $3/2$, respectively and the problem with $\ell \ll 1$ can be rescaled into that with $\ell = 1$ without changing probabilities.

It is clear by symmetry that $\text{Prob}\{\textit{Left}\}$ and $\text{Prob}\{\textit{Right}\}$ have the same scaling in ℓ. Let us concentrate on $\text{Prob}\{\textit{Right}\}$. We can write the equation for the half line Γ_+ in the form

$$\Gamma_+ : a \mapsto \varphi(a_2) + \delta\ell^{3/2} + \left(\partial_a\varphi(a_2) + \gamma\ell^{1/2}\right)(a - a_2), \tag{5.3}$$

where γ and δ are positive $O(1)$ quantities. Hence, introducing $\alpha \equiv a - a_2$, the condition *Right* can be written to the leading order as

$$\int_0^\alpha \left(u_0(a) + \gamma\ell^{1/2}\right) \mathrm{d}a + \delta\ell^{3/2} + \frac{\alpha^2}{2} > 0, \text{ for all } \alpha > 0. \tag{5.4}$$

By the change of variable $\alpha = \beta\ell$ and use of the fact that the Brownian motion has scaling exponent $1/2$, one can write the condition *Right* as

$$\int_0^\beta (u_0(a) + \gamma)\, \mathrm{d}a > -\delta, \text{ for all } \beta \in [0, \ell^{-1}]. \tag{5.5}$$

Without affecting the leading order, one can replace the Brownian motion by a stepwise constant random walk with jumps of ± 1 at integer a's. The integral in (5.5) has a geometric interpretation, as highlighted in Figure 20, which shows a random walk starting from the ordinate γ and the arches determined by successive zero-passings. The areas of these arches are denoted $S_\star, S_1, ...S_n, S_{\star\star}$. It is easily seen that

$$\text{Prob}\{\textit{Right}\} \sim \text{Prob}\{S_1 > 0, S_1 + S_2 > 0, ..., S_1 + ... + S_n > 0\}, \tag{5.6}$$

where $n = O(\ell^{-1/2})$ is the number of zero-passings of the random walk in the interval $[0, \ell^{-1}]$. The probability (5.6) can be evaluated by random walk methods (see, *e.g.* [43], Chap. 12, Sect. 7), yielding

$$\text{Prob}\{\textit{Right}\} \sim \text{Prob}\{n \text{ first sums} > 0\} \propto n^{-1/2} \propto \ell^{1/4}. \tag{5.7}$$

By (5.1, 5.2) and (5.7), the probability to have a regular point in a small interval of length ℓ behaves as $\ell^{1/2}$ when $\ell \to 0$. Thus, the regular points have a box-counting dimension $1/2$.

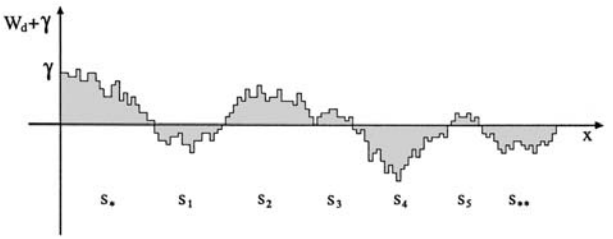

Fig. 20. The arches construction which uses the zero-passings of a random walk to estimate the integral of Brownian motion (from Refs. [7, 42]).

6 Preshocks and the pdf of velocity gradients in one dimension

In this section we shall determine the tail behavior of the probability density function (pdf) of the velocity gradient for one-dimensional decaying burgulence. To explain some of the motivations for this study, it is useful to make a digression concerning the forced one-dimensional Burgers equation:

$$\partial_t u + u\partial_x u = \nu\partial_{xx} u + f(x,t), \tag{6.1}$$

$$u(x,t_0) = u_0(x). \tag{6.2}$$

The latter displays much richer features than the unforced problem. The case where the force is random has often been studied as a prototype for a wide range of problems in non-equilibrium statistical physics (see Sect. 1.2).

Equation (6.1) can also be used in the same spirit as the forced Navier–Stokes equation, namely to investigate universality of various statistical properties with respect to the forcing. For Navier–Stokes turbulence, when the force is confined to large spatial scales and the Reynolds number is very high, small-scale (inertial range) statistical scaling properties are generally conjectured not to depend on the forcing, except through overall numerical factors. Similar conjectures have been made for burgulence with large-scale forcing. For example, there is little doubt that, because of the presence of shocks, structure functions of order $p > 1$ have universal exponents equal to unity, as in the decaying case (see, *e.g.* [16, 44]). More controversial is the tail behavior of the probability density function (pdf) of velocity gradients and velocity increments in the limit of zero viscosity when the force is a white-noise process in time. For increments, the problem was addressed for the first time by Chekhlov and Yakhot [45], who considered a force with a power-law spectrum, acting both at large and at small scales. Concerning the pdf $p(\xi)$ at large negative gradients ξ, it is generally believed that it follows a power law

$$p(\xi) \propto |\xi|^{\alpha}, \quad \text{for } \xi \to -\infty, \tag{6.3}$$

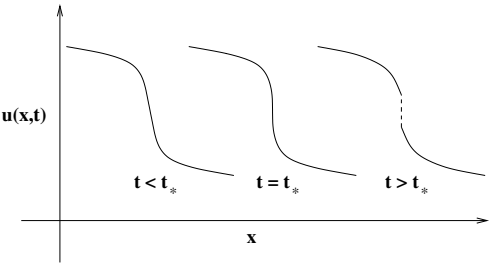

Fig. 21. Eulerian structure of the solution just before a preshock, at the time $t_\star$ of a preshock and just after.

but the conjectured values of α differ markedly. Polyakov [46] and Boldyrev [47], using a field-theoretical operator product expansion, predicted $\alpha = -5/2$; E *et al.* [44], using a semi-heuristic approach in which preshocks (nascent shocks) are key, predicted $\alpha = -7/2$; Gotoh and Kraichnan [48], using a Fokker–Planck equation approach, predicted $\alpha = -3$; more recent work by Kraichnan [49] favored $\alpha = -7/2$. E and Vanden Eijnden [50, 51] developed a probabilistic formalism adapted to solutions with shocks and giving insight into many aspects of the problem; they proved that $\alpha < -3$, and made a good case for $\alpha = -7/2$. The question of the correct law for the case of white-noise forcing remains however open (we shall come back to this later).

Actually, there is a situation much simpler than that originally considered in [44], for which the argument in favor of $\alpha = -7/2$ can be made rigorous, namely decaying burgulence. This closes our digression; in the remainder of this section we concentrate on the the unforced problem

$$\partial_t u + u\partial_x u = \nu\partial_x^2 u, \tag{6.4}$$

in the limit of vanishing viscosity $\nu \to 0$ and we follow references [52,53]. We assume a random initial velocity $u_0 = -(\mathrm{d}\psi_0/\mathrm{d}a)$, deriving from a smooth initial potential. Homogeneity is not required. The value $\alpha = -7/2$ for the exponent of the pdf at large negative gradients is easily understood in this case. It is just the signature of the preshocks, the cubic root singularities in Eulerian coordinates, which appear when new shocks are created (see Fig. 21). Preshocks constitute discrete events in space-time, contrary to shocks which persist in time (until they merge). These preshocks are the only structures giving large *finite* negative gradients: shocks give infinite negative gradients (unless a finite viscosity is introduced) and the gradients in the immediate spatial neighborhood of a mature shock are not particularly large. A simplified presentation is given hereafter for the case of a

single preshock; the contributions of several preshocks to the pdf are just additive.

Let us suppose that the initial gradient $\mathrm{d}u_0/\mathrm{d}a$ has a minimum at $a = 0$ (corresponding to an inflection point with negative derivative of the initial velocity), so that a shock will appear at time $t = t_\star = -1/((\mathrm{d}u_0/\mathrm{d}a)(0))$ and at $x = t_\star u_0(0)$. Without loss of generality, we assume $u_0(0) = 0$ (otherwise we perform a Galilean transformation to bring it to zero). As the initial velocity is supposed to be sufficiently smooth, we can perform a Taylor expansion of the initial potential in the neighborhood of $a = 0$. We then have, locally,

$$\psi_0(a) = c_1 a^2 - c_2 a^4 + \text{h.o.t.}, \tag{6.5}$$

where c_1 and c_2 are positive (random) constants and "h.o.t." stands for higher-order terms. The Lagrangian potential is locally

$$\varphi = -\frac{a^2}{2} + t\psi_0(a) = \frac{\tau}{2}a^2 - tc_2 a^4 + \text{h.o.t.}, \tag{6.6}$$

where $\tau = (t - t_*)/t_*$. The Lagrangian map outside the shock is thus

$$x(a,t) = -\partial_a \varphi(a,t) = -\tau a + 4tc_2 a^3 + \text{h.o.t.} \tag{6.7}$$

The Lagrangian potential, together with its convex hull, are shown in Figure 22. It is convex for $t \le t_\star$. At $t = t_\star$, there is a degenerate maximum with quartic behavior, and, immediately after t_* (for $\tau > 0$), convexity is lost and a shock interval is born. Given the symmetry, resulting from our choice of coordinates, the convex hull contains a horizontal segment extending between the two maxima $a_\pm = \pm(\tau/(4c_2))^{1/2}$. The velocity gradient

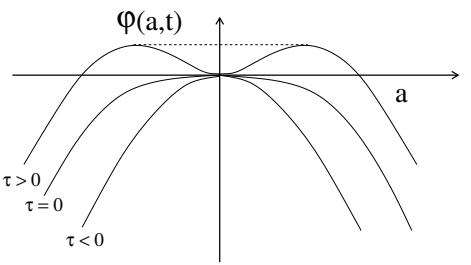

Fig. 22. Normal form of the Lagrangian potential in the neighborhood of a preshock in one dimension. At the time of the preshock ($\tau = (t - t_*)/t_* = 0$), the Lagrangian potential changes from a single extremum to three extrema and develops a non-trivial convex hull (shown as a dashed line).

can be written locally as

$$\partial_x u(x,t) = \frac{(\mathrm{d}u_0/\mathrm{d}a)(a)}{\partial_a x(a,t)} = \frac{2/t_\star}{-\tau + 12c_2 a^2}, \tag{6.8}$$

where a is the unique preimage of x by the naive Lagrangian map outside of the shock interval $]a_-, a_+[$. Since, by (6.7), the relation between x and a is cubic at $\tau = 0$, the velocity gradient $\partial_x u(x, t_\star) \propto |x|^{-2/3}$, which is unbounded. For any $t \neq t_\star$, the gradient remains bounded, except at the shock location. For $\tau < 0$, just before creation of the shock, the cubic relation between x and a still holds, except in a region of Lagrangian width of the order of $\tau^{1/2}$, and hence of Eulerian width $\sim \tau^{3/2}$, where the relation becomes linear to leading order.

The question is now: what is the fraction of Eulerian space-time where $\partial_x u < \xi$, with ξ a large negative number? Because of the cubic root structure, x must be in a small interval of width $\sim |\xi|^{-3/2}$. The time must be sufficiently close to $t_\star$ for this interval still to be in the region of validity of the cubic relation, that is, within $\sim |x|^{2/3} \sim |\xi|^{-1}$. Hence, the relevant space-time fraction or, in other words, the cumulative probability to have $\partial_x u < \xi$ is proportional to $|\xi|^{-5/2}$. This gives a pdf $p(\xi) \propto |\xi|^{-7/2}$ at large negative ξ's.

Actually, there is another contribution, also proportional to $|\xi|^{-7/2}$ stemming from a small time interval $\tau \sim |x|^{2/3} \sim |\xi|^{-1}$ just *after* $t_\star$ when small-amplitude shocks are present which have not yet completely destroyed the cubic root structure (see Ref. [52]). Similar arguments can be used to show that there are power-law ranges with exponent $-7/2$ and $+1$ in the pdf of velocity increments for decaying burgulence [52].

The preshock argument has first been introduced phenomenologically in [44] to predict pdf's of velocity gradients and increments for the case of white-noise in time forcing at large scales. In principle, in the presence of forcing, spatio-temporal accumulations of preshocks, invalidating the $-7/2$ law, cannot be ruled out. Nevertheless, numerical evidence in favor of the $-7/2$ law has been recently obtained by one of us (JB), using particle tracking simulations with a shot-noise approximation to white noise.

7 The pdf of density

In cosmological applications of the adhesion model/Burgers equation, it is of special interest to analyze the behavior of the density of matter, since the large-scale structures may also be characterized as mass condensations. In Eulerian coordinates, the mass density ρ satisfies the continuity equation

$$\partial_t \rho + \nabla \cdot (\rho \mathbf{v}) = 0. \tag{7.1}$$

The initial density is denoted by $\rho_0(\mathbf{a})$.

The question we intend to address here is the behavior, in the limit of vanishing viscosity and at large ρ's, of the pdf of mass density $p(\rho)$, when the initial velocity is random and smooth (and not necessarily homogeneous). This problem was studied in [53], where it was shown that density pdf's have universal power-law tails with exponent $-7/2$ in any dimension. This behavior stems from singularities, other than shocks, whose nature is quite different in one and several dimensions. (Similar results can in principle be obtained for velocity gradients and increments which are, however, not scalars in more than one dimension.)

In one dimension, the pdf of the mass density at large arguments is basically the same as the pdf of gradients at large negative arguments. Indeed, it is easy to show that, for any x not at a shock location,

$$\rho(x,t) = \rho_0(a)\,(1 - t\partial_x u(x,t))\,, \tag{7.2}$$

where a is the preimage of x by the Lagrangian map [3]. If now ρ_0 is bounded from below and above (*e.g.*, for uniform ρ_0), the result of the previous section implies that, for $\rho \to \infty$, the pdf $p(\rho)$ of the mass density satisfies a $\rho^{-7/2}$ law, which is again the signature of preshocks.

The key to studying this problem in more than one dimension is the geometric construction of the solution via the convex hull of the Lagrangian potential (see Sect. 2.3). Conservation of mass (7.1) implies that the density is given at regular points by

$$\rho(\mathbf{x},t) = \frac{\rho_0(\mathbf{a})}{J(\mathbf{a},t)}, \tag{7.3}$$

where J is the Jacobian of the Lagrangian map. (The density is infinite within shocks.) Since the Jacobian is (up to a factor $(-1)^d$) equal to the Hessian of the Lagrangian potential (determinant of the matrix of second space derivatives), it follows that large densities are typically obtained only near parabolic points (where the Hessian vanishes). However, arbitrarily close to a parabolic point there are generically hyperbolic points where the surface defined by φ crosses its tangent (hyper)plane and which, therefore, do not belong to its convex hull. Yet, there exist in general exceptional "kurtoparabolic" points which are parabolic and belong to the boundary of the set of regular points (*kurtos* means convex in Greek). Near such points, arbitrarily large densities are obtained. In one dimension, the only kurtoparabolic points are the preshocks which are discrete space-time events in both Eulerian and Lagrangian coordinates. In two and more dimensions, kurtoparabolic points are also born at preshocks but live in general for a finite time; they reside on manifolds of spatial dimension $(d-1)$ (see

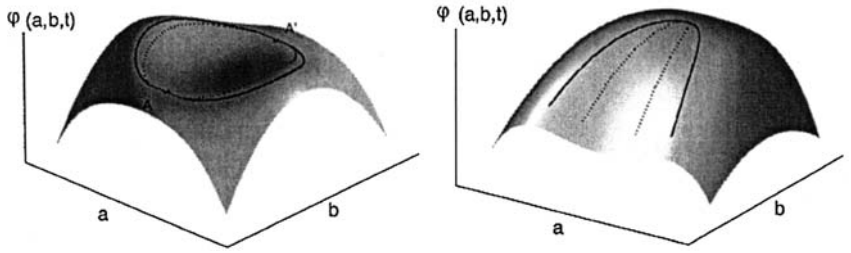

Fig. 23. Lagrangian potential in two dimensions with (a, b) coordinates, just after a preshock (left) and in the immediate neighborhood of a kurtoparabolic point (right). Continuous lines: separatrices between the regular part and the ruled surfaces of the convex hull; dotted-lines: vanishing of the Jacobian of the Lagrangian map. A and A' are a pair of kurtoparabolic points born with the shock.

Fig. 7). In Eulerian space, they are associated to boundaries of shocks (*e.g.* end points of shock lines for $d = 2$).

The determination of the large-ρ tail of the cumulative probability distribution of the density, $P^{>}(\rho)$, is equivalent to finding the fraction of Eulerian space-time where ρ exceeds a given value (see Ref. [53] for details). The latter is determined by changing from Eulerian to Lagrangian coordinates and Taylor-expanding to the relevant order the Lagrangian potential near a kurtoparabolic point, in a suitable coordinate frame:

$$\varphi(\mathbf{a}, t) \simeq \zeta a_1^4 + \sum_{j>1} \left[-\frac{\mu_j}{2} a_j^2 + \beta_j a_1^2 a_j \right]. \tag{7.4}$$

From (7.4), it is then easy to determine explicitly the line of vanishing Jacobian, the separatrix of the convex hull and the area where the density exceeds the value ρ (as illustrated in Fig. 24 for the 2-D case).

When $\rho \to \infty$, the cumulative probability can be estimated as follows

$$P^{>}(\rho) \propto \underbrace{\rho^{-3/2}}_{\text{from } a_1} \times \underbrace{\rho^{-1}}_{\text{from } a_2} \times \underbrace{1 \times \ldots \times 1}_{\text{from } a_3 \ldots a_d} \times \underbrace{1}_{\text{from time}} . \tag{7.5}$$

Hence, the cumulative probability $P^{>}(\rho) \propto \rho^{-5/2}$ in any dimension; so that the pdf of the mass density has a universal power-law behavior with exponent $-7/2$. We have seen that the theory is rather different in one dimension and higher dimensions, because kurtoparabolic points are persistent only in the latter case. However, the scaling law for the resulting pdf is the same in all dimensions. Actually, two orthogonal spatial directions, a_1 and a_2 in (7.5), play the same role as space and time in one dimension.

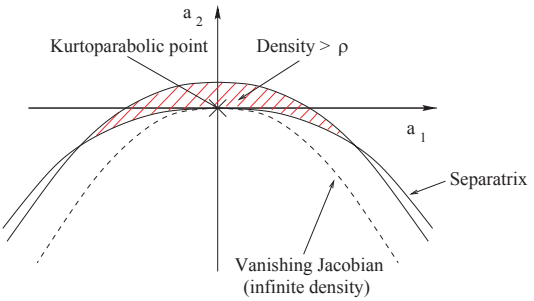

Fig. 24. Projection in the two-dimensional case of the neighborhood of a kurtoparabolic point.

It is now clear that, for burgulence, the algebraic tails of the pdf of velocity gradients or of the density stem from singularities. Turning briefly to *incompressible three-dimensional Navier–Stokes turbulence*, we note that measurements of pdf's for space or time derivatives of Eulerian velocities have not yet revealed power-law tails, but such tails may just have been, so far, "lost in the experimental noise". There has indeed been considerable speculations about singularities of the Navier–Stokes equations in the inviscid limit [19]. If singularities with divergent gradients are present, they will give power-law tails, at least as intermediate asymptotics when the viscosity is small (the converse is however not true, since statistical effects not related to singularities can also give power laws). The confirmed absence of power laws would probably rule out singularities.

8 Kicked burgulence

8.1 Forced Burgers equation and variational formulation

In the limit of vanishing viscosity and when no force is applied, the Burgers equation just means that fluid particles keep their initial velocity until they stick together in a shock. So, until merger, the position $X(t)$ of a given fluid particle will depend linearly on time:

$$X(t) = X(t_0) + (t - t_0)u_0(X(t_0)), \quad u(X(t), t) = u_0(X(t_0)). \tag{8.1}$$

When a force is applied, fluid particles trajectories, before merger with a shock, follow forcing-dependent continuous trajectories governed by

$$\frac{\mathrm{d}^2}{\mathrm{d}t^2}X(t) = f(X(t), t), \quad \frac{\mathrm{d}}{\mathrm{d}t}X(t) = u(X(t), t); \tag{8.2}$$

thus their dynamics can be rather complex (see Fig. 25).

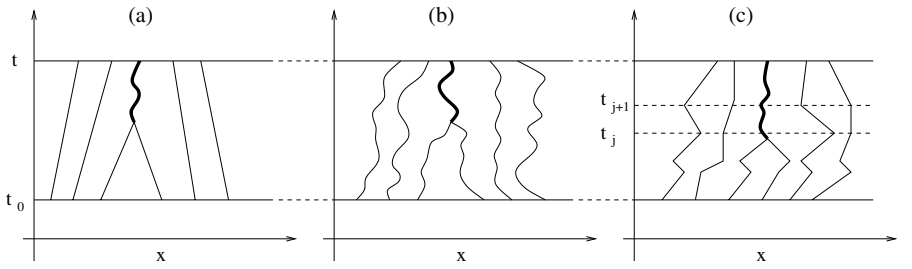

Fig. 25. Trajectories of particles in the decaying case (a), in the continuously forced case (b) and in the kicked case (c). The thick lines are shock trajectories.

Following reference [30], we shall be concerned here with the one-dimensional case where the force is a sum of impulses (or kicks), concentrated at discrete times t_j's:

$$f(x,t) = \sum_{j>j_0} f_j(x)\delta(t-t_j), \tag{8.3}$$

where $t_{j_0} = t_0$ is the initial time, and t_{j_0+1} is the time of the first kick. The kicking times t_j's and the kick $f_j(\cdot)$'s are prescribed. They can be either fixed or random. The meaning of such a forcing is that, between kicks, we let the solution evolve as a solution of the unforced problem. At each kicking time t_j, we discontinuously change the velocity field by the amount $f_j(x)$:

$$u(x,t_{j+}) = u(x,t_{j-}) + f_j(x). \tag{8.4}$$

This is an intermediate case between decay and time-continuous forcing. Such forcing implies a piecewise-linear time dependence of the position of a given fluid particle (see Fig. 25).

It is of interest to notice that this kind of discrete-in-time forcing can be applied also to the Navier–Stokes equations, with features of decaying turbulence still present to some extent. The original motivation for introducing such a forcing was to approximate white-noise-in-time forcing by discrete random noise, also called shot noise. But actually, the kicked case displays interesting features of its own. As will be shown later, the problem can be understood in terms of area-preserving mappings to which we can apply KAM theory (see Ref. [54] and references therein) and Aubry–Mather theory [55, 56].

We will focus on the space-periodic case. Namely, we assume that both the initial condition $u_0(\cdot)$ and the kicks $f_j(\cdot)$ are periodic with period 1, with respect to the space variable. For the moment, let us also assume that the initial velocity and the kicks both have zero spatial mean value over

the space period $[0,1[$. Since the mean velocity is conserved by Burgers dynamics, we have

$$\int_0^1 u(x,t)\mathrm{d}x = 0 \tag{8.5}$$

at all times. This constraint implies that the velocity potential $\psi(x,t)$, defined by $u(x,t) = -\partial_x \psi(x,t)$, is itself periodic in space. Let us define the kicking potentials $F_j(\cdot)$, so that

$$f_j(x) = -\frac{\mathrm{d}}{\mathrm{d}x} F_j(x). \tag{8.6}$$

It is then easy to write the potential at any time t, using between successive kicks the standard maximum representation (2.3) for decaying solution in the limit of vanishing viscosity (this is reexpressed here as a minimum in order to minimize a suitable action function), to obtain

$$\psi(x,t) = -\min_{y_J} \left[\frac{(x-y_J)^2}{2(t-t_J)} - \psi(y_J, t_{J-}) - F_J(y_J) \right], \tag{8.7}$$

where the index J is such that $t_J < t \le t_{J+1}$. Repeating this step as often as necessary to work our way back to the initial time, we obtain

$$\psi(x,t) = -\min_{\{y_j\}_{j_0 \le j \le J}} \left[A\left(x,t;\{y_j\}\right) - \psi_0(y_{j_0}) \right], \tag{8.8}$$

where A is an action which has to be minimized,

$$A\left(x,t;\{y_j\}\right) = \frac{(x-y_J)^2}{2(t-t_J)} + \sum_{j=j_0}^{J-1} \left[\frac{(y_{j+1}-y_j)^2}{2(t_{j+1}-t_j)} - F_{j+1}(y_{j+1}) \right]. \tag{8.9}$$

There is a similar representation for the case where the forcing $f(x,t) = -\partial_x F(x,t)$ is continuously applied, namely

$$\psi(x,t) = -\min_{y(\cdot)} \left[A\left(x,t;y(\cdot)\right) - \psi_0(y(t_0)) \right]. \tag{8.10}$$

The minimum is now taken over continuous curves $y(\cdot)$ such that $y(t) = x$, the action being given by

$$A\left(x,t;y(\cdot)\right) = \int_{t_0}^{t} \left[\frac{1}{2}(\dot{y}(s))^2 - F(y(s),s) \right] \mathrm{d}s. \tag{8.11}$$

This representation goes back to work by Oleinik [57] on general conservation laws. It can be derived as the continuous limit of the discrete formulation when letting the time between kicks tend to zero. Many features of

the forced Burgers equation were obtained by E *et al.* [58]. As we will see, the key notions introduced by E *et al.*, such as minimizers, global minimizer and main shock, are still valid in the case of discrete-in-time forcing.

First, we will introduce the notion of minimizing sequence (or minimizer). In terms of fluid particles trajectories, the minimum representation (8.8) just means that, to obtain the solution at time t and at some Eulerian location x, one has to look at all possible trajectories reaching x, and choose between them those which minimize the action. The sequence for which the minimum is achieved is, by definition, a minimizer. In general, there is only one minimizing trajectory arising at a given x. But for a countable set of x-values, there are several minimizing trajectories. These correspond to particles coalescing in a shock.

A minimizer can be explicitly characterized by requiring the vanishing of the derivatives, with respect to all the y_j's, of the argument of the minimum in (8.8). A minimizing sequence then has to verify the following Euler–Lagrange equations:

$$v_{j+1} = v_j + f_j(y_j), \tag{8.12}$$

$$y_{j+1} = y_j + (t_{j+1} - t_j)\,[v_j + f_j(y_j)]\,, \tag{8.13}$$

where $v_j \equiv (y_j - y_{j-1})/(t_j - t_{j-1})$ is the velocity at the location y_j just before the kick. These equations have to be supplemented by the following initial and final conditions:

$$v_{j_0} = u_0(y_{j_0}), \tag{8.14}$$

$$x = y_J + (t - t_J)v_{J+1}. \tag{8.15}$$

Note that $v_{J+1} = u(x,t)$. The Euler–Lagrange map is area-preserving. It is also explicitly invertible, so that for a given (x,v), one can reconstruct the past history of a particle, except if a shock sits at x.

8.2 Periodic kicks

From now, we will focus on a particular case of forcing which displays globally the same features as random forcing but is much easier to handle. Namely, following reference [30], we consider the case of time-periodic kicks: the kicking potential is the same at each kick, $F_j(x) = G(x)$ for all j, and

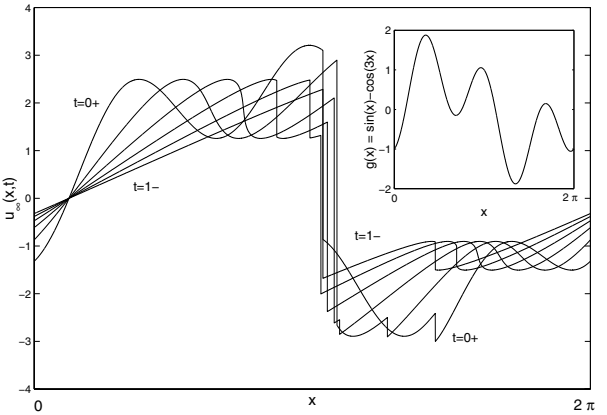

Fig. 26. Snapshots over one time period of the velocity for the limiting solution corresponding to the kicking force $g(x) = \sin x - \cos(3x)$ on the space period $[0, 2\pi[$ (see upper inset). The main shock is located around $x = \pi$; the global minimizer, here a fixed point, is the point of vanishing velocity common to all curves. Notice that during each period, two new shocks are born and two mergers occur.

the time interval is constant, $t_{j+1} - t_j = 1$, for convenience. The force can then be written

$$f(x,t) = \sum_{j>j0} g(x)\delta(t-j), \tag{8.16}$$

where $g = -\mathrm{d}G/\mathrm{d}x$.

We now show, following reference [30], that the solution to the Burgers equation with this kind of forcing converges exponentially fast in time to a periodic solution $u_\infty(x,t)$. Snapshots of the time-periodic solution for one instance of kicking are shown in Figure 26; Figure 27 shows the exponential relaxation to $u_\infty(x,t)$.

Actually, the convergence to a unique solution at long times is related to properties near a fixed point of the two-dimensional dynamical system defined by the Euler–Lagrange map which reads here

$$v_{j+1} = v_j + g(y_j), \tag{8.17}$$

$$y_{j+1} = y_j + v_j + g(y_j). \tag{8.18}$$

A fixed point $(y_\star, v_\star)$, obviously, satisfies $v_\star = 0$ and $g(y_\star) = 0$. The latter expresses that the kicking potential achieves an extremum at $x = y_\star$. Let $P = (x_\mathrm{c}, 0)$ be the particular fixed point of the map (8.17, 8.18), which corresponds to the location where the forcing potential achieves its maximum over the space period. This point is hyperbolic because the linearized

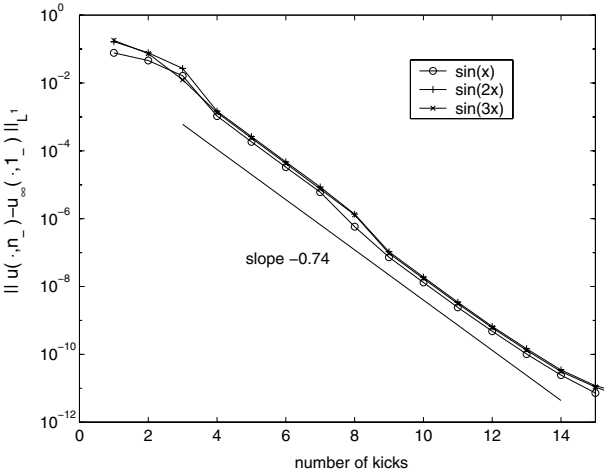

Fig. 27. Exponential relaxation to a time-periodic solution for the same forcing as in Figure 26, with three different initial conditions, as labeled. $\int_0^{2\pi} |u(x, n_-) - u_\infty(x, 1_-)| \mathrm{d}x/(2\pi)$ is plotted vs the number of kicks.

system in its neighborhood has two real eigenvalues $\lambda > 1$ and $1/\lambda$, where

$$\lambda = 1 + c + \sqrt{c^2 + 2c}, \quad c = -\frac{1}{2}\frac{\mathrm{d}^2}{\mathrm{d}x^2} G(x_\mathrm{c}). \tag{8.19}$$

In the phase space (x, v), two globally invariant curves are associated to the corresponding eigendirections. These are (i) the stable manifold $\Gamma^{(\mathrm{s})}$, associated to $1/\lambda$, which is the set of points (x, v) converging to the fixed point under iteration of the map (because the eigenvalue is less than one), and (ii) the unstable manifold $\Gamma^{(\mathrm{s})}$, associated to λ, and generated by inverse iteration (see Fig. 28). An arbitrary continuous curve in the (x, v) plane which intersects the stable manifold will, under iteration, converge exponentially fast to the unstable manifold at the rate $1/\lambda$.

In the language of Burgers dynamics, the curve in the (x, v) plane defined by an initial condition $u_0(x)$ will be mapped after some kicks into a curve very close to the unstable manifold. To understand this mechanism of convergence, let us take an initial time t_0 tending to $-\infty$ and look at the behavior of the solution at time $t = 0$. The trajectory of the hyperbolic fixed point P corresponds to the so-called global minimizer. The global minimizer is the trajectory of a fluid particle never to be absorbed by a shock. Such a global minimizer is unique, and every minimizing trajectory converges exponentially fast to the global minimizer as $t \to -\infty$ [58]. This is illustrated in Figure 29a. By definition of the unstable manifold, each

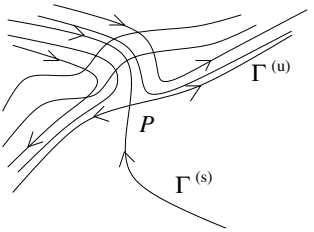

Fig. 28. Sketch of a hyperbolic fixed point P with its stable ($\Gamma^{(s)}$) and its unstable ($\Gamma^{(u)}$) manifolds. A curve, which intersects $\Gamma^{(s)}$, will eventually converge to $\Gamma^{(u)}$ under iteration of the map.

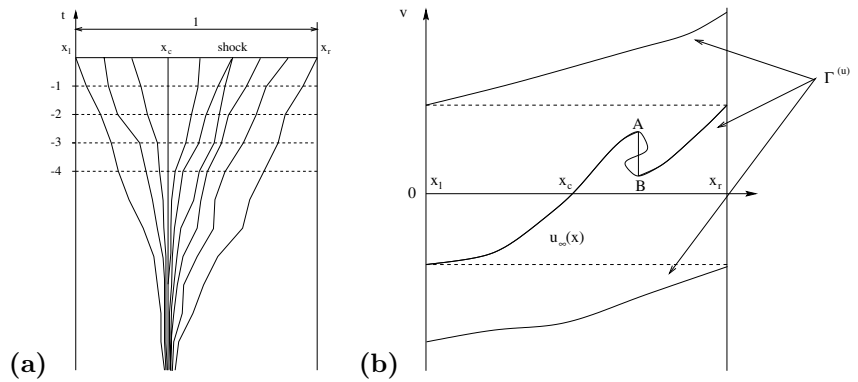

Fig. 29. (a) Minimizers on the (x,t) cylinder; initial time t_0 is taken at $-\infty$. Shock locations are characterized by having two minimizers (an instance is at x_1); the fat line $x = x_c$ is the global minimizer. (b) Unstable manifold $\Gamma^{(u)}$ on the (x,v) cylinder which passes through the fixed point $P = (x_c, 0)$; the bold line is the graph of the limiting periodic solution. The main shock is located at $x_l = x_r$, and another shock at x_1 corresponds to a local zig-zag of $\Gamma^{(u)}$ between A and B.

point (y_j, v_j) of a minimizer belongs thus to $\Gamma^{(u)}$ and every regular part of the graph of the limiting velocity belongs to the unstable manifold. Now we turn to the construction of the main shock. Since $\lambda > 0$, every minimizing trajectory starting from a point on the right (resp. left) of the global minimizer approaches it as $t \to -\infty$ from the right (resp. left). Hence, there exists x_r (resp. x_l), the rightmost (resp. leftmost) location from which a minimizer approaches the global minimizer from the right (resp. left). By periodicity in space and uniqueness of the global minimizer, these two points are actually the same: $x_r = x_l \bmod 1$. If we shift the periodicity interval to $[x_l, x_r]$, we can draw $\Gamma^{(u)}$ on the (x,v)-cylinder. The regular parts of the

limiting solution belong to this graph. By construction there is thus a shock at $x = x_{\rm l} = x_{\rm r}$ (see Fig. 29b). This is the *main shock*, the unique shock which exists for an infinite time. In Burgers dynamics, shocks are born and then they may merge. The main shock is a shock which has always existed when letting the initial time tend to $-\infty$. The other shocks are associated to the regions where $\Gamma^{(\rm u)}$ is multi-valuated in x. Their locations are determined by requiring that the action be the same at points such as A and B in Figure 29b.

8.3 Connections with Aubry–Mather theory

So far, we have exclusively considered zero-mean-value initial conditions. Let us briefly consider the case where

$$\int_0^1 u(x,t)\mathrm{d}x = \int_0^1 u_0(x)\mathrm{d}x = a > 0. \tag{8.20}$$

The Burgers problem is then in exact correspondence with the description of equilibrium states of the Frenkel–Kontorova model [59]. In the latter, one has a one-dimensional chain of atoms connected by elastic springs in the presence of a space-periodic potential. The potential energy, which must be minimized to obtain the (classical) ground state, is

$$H(\{y_j\}) = \sum_j \frac{1}{2}\left(y_{j+1} - y_j - a\right)^2 - G(x), \tag{8.21}$$

where a is the unstretched distance between atoms. This problem was investigated by Aubry [55] and Mather [56]. The representation (8.21) matches the action minimizing representation for Burgers equation with a mean velocity a. The connection between the forced Burgers equation and Aubry–Mather theory was investigated by Jauslin *et al.* [60], E [61] and Sobolevski [62].

For $a = 0$, the global minimizer is a trivial ground state, associated to a fixed point, but for $a \neq 0$, it is much more complex. Within some intervals of the parameter a, the global minimizer lives on a periodic orbit associated to a rational rotation number ρ (asymptotic slope of the trajectory when $t \to -\infty$). The graph of ρ as a function of a is actually a Devil's staircase. The transitions between the intervals of the mean velocity corresponding to rational rotation numbers display interesting phenomena, such as accumulations of shocks (see Fig. 30).

We are grateful to V. Arnold, M. Blank, I.A. Bogaevski, G. Eyink, J.D. Fournier, W. E, K. Khanin, J. Lukovich, R. Mohayaee, Ya. Sinai, M.R. Rahimi Tabar, E. Vanden Eijnden, A. Sobolevski, M. Vergassola, B. Villone for useful comments. Part of this work was done

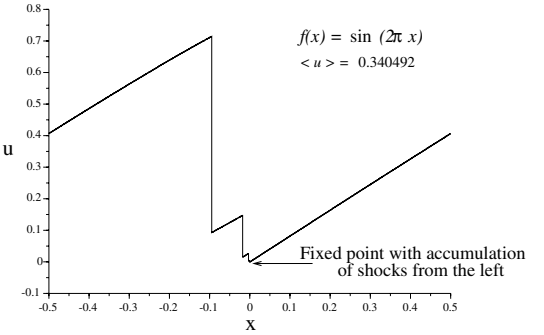

Fig. 30. Velocity profile at the first transition to a rational nonvanishing rotation number when increasing the mean velocity $a = \langle u \rangle$ from 0. Note the accumulation of shocks.

while JB and UF were visiting the Center of Nonlinear Studies (Los Alamos, U.S.A.) and the Isaac Newton Institute (Cambridge, U.K.); their support is gratefully acknowledged. This work was also supported by the European Union under contract HPRN-CT-2000-00162.

References

[1] E. Hopf, *Comm. Pure Appl. Math.* **3** (1950) 201-230.

[2] J.D. Cole, *Quart. Appl. Math.* **9** (1951) 225-236.

[3] S.N. Gurbatov, A.N. Malakhov and A.I. Saichev, *Non-linear Random Waves and Turbulence in Nondispersive Media: Waves, Rays, Particles* (Manchester University Press, Manchester, 1991).

[4] Y.B. Zel'dovich, *Astron. Astrophys.* **5** (1970) 84-89.

[5] S.N. Gurbatov and A.I. Saichev, *Radiophys. Quant. Electr.* **27** (1984) 303-313.

[6] Z. She, E. Aurell and U. Frisch, *Comm. Math. Phys.* **148** (1992) 623-641.

[7] M. Vergassola, B. Dubrulle, U. Frisch and A. Noullez, *Astron. Astrophys.* **289** (1994) 325-356.

[8] P.J.E. Peebles, *Principles of Physical Cosmology* (Princeton University Press, Princeton, 1993).

[9] P. Coles and F. Lucchin, *Cosmology: The Origin and Evolution of Cosmic Structures* (J. Wiley and Sons, Chichester, 1995).

[10] V.I. Arnold, S.F. Shandarin and Y.B. Zel'dovich, *Geophys. Astrophys. Fluid Dynam.* **20** (1982) 111-130.

[11] L. Kofman, E. Bertschinger, J. Gelb and A. Nusser, *Astrophys. J.* **420** (1994) 44-57.

[12] D. Chowdhury, L. Santen and A. Schadschneider, *Phys. Rep.* **329** (2000) 199-329.

[13] M. Kardar, G. Parisi and Y.-C. Zhang, *Phys. Rev. Lett.* **56** (1986) 889-892.

[14] A.L. Barabási and H.E. Stanley, *Fractal Concepts in Surface Growth* (Cambridge University Press, Cambridge, 1995).

[15] M. Kardar and Y.-C. Zhang, *Phys. Rev. Lett.* **58** (1987) 2087-2090.

[16] J.P. Bouchaud, M. Mézard and G. Parisi, *Phys. Rev. E* **52** (1995) 3656-3674.

[17] S.A. Orszag, *Statistical Theory of Turbulence*, in Fluid Dynamics, Les Houches 1973, edited by R. Balian and J.L. Peube (Gordon and Breach, New York, 1977) pp. 237-374.

[18] H.A. Rose and P.L. Sulem, *J. Phys. France* **39** (1978) 441-484.

[19] U. Frisch, *Turbulence: The Legacy of A.N. Kolmogorov* (Cambridge University Press, Cambridge, 1995).

[20] M. Lesieur, *Fluid Mechanics and Its Applications* **40** (Kluwer, 1997).

[21] F. Calogero, *Lett. Nuovo Cimento* **13** (1975) 411-416.

[22] U. Frisch and R. Morf, *Phys. Rev. A* **23** (1981) 2673-2705.

[23] J.D. Fournier and U. Frisch, *J. Méc. Théor. Appl.* **2** (1983) 699-750.

[24] P.-D. Lax, *Comm. Pure Appl. Math.* **10** (1957) 537-566.

[25] U. Frisch and R. Bourret, *J. Math. Phys.* **11** (1970) 364-390.

[26] L.D. Landau and E.M. Lifshitz, *Statistical Physics* (Butterworth-Heinemann, Oxford, 1980).

[27] I.A. Bogaevski, *Singularities of convex hulls as fronts of Legendre varieties*, in Geometry and Topology of Caustics – Caustics '98, Banach Center publications **50** (1999) 61-74, Institute of Mathematics, Polish Academy of Sciences (Warsaw).

[28] F. Aicardi, On the classification of generic phenomena in thermodynamic binary mixtures, *Physica D* (2001) (submitted).

[29] A. Noullez and M. Vergassola, *J. Sci. Comput.* **9** (1994) 259-281.

[30] J. Bec, U. Frisch and K. Khanin, *J. Fluid Mech.* **416** (2000) 239-267.

[31] T. von Kármán and L. Howarth, *Proc. R. Soc. Lond. A* **164** (1938) 192-215.

[32] A.N. Kolmogorov, *Dokl. Akad. Nauk SSSR* **31** (1941) 538-540.

[33] I. Proudman and W.H. Reid, *Phil. Trans. R. Soc. Lond. A* **247** (1954) 163-189.

[34] S.N. Gurbatov, S.I. Simdyankin, E. Aurell, U. Frisch and G. Toth, *J. Fluid Mech.* **344** (1997) 339-374.

[35] J.M. Burgers, *The Nonlinear Diffusion Equation* (D. Reidel, Dordrecht, 1974).

[36] S. Kida, *J. Fluid Mech.* **93** (1979) 337-377.

[37] S.A. Molchanov, D. Surgailis and W.A. Woyczynski, *Comm. Math. Phys.* **168** (1995) 209-226.

[38] G.L. Eyink and J. Xin, *J. Stat. Phys.* **100** (2000) 679-741.

[39] G.L. Eyink and D.J. Thomson, *Phys. Fluids* **12** (2000) 477-479.

[40] S. Ossia and M. Lesieur, *J. Turbulence* **1** (2000) 007.

[41] M. Chaves, G. Eyink, U. Frisch and M. Vergassola, *Phys. Rev. Lett.* **86** (2001) 2305-2308.

[42] Ya. Sinai, *Comm. Math. Phys.* **148** (1992) 601-622.

[43] W. Feller, *An Introduction to Probability Theory and its Applications*, Vol. 2 (J. Wiley and Sons, Chichester, 1995).

[44] W. E, K. Khanin, A. Mazel and Ya. Sinai, *Phys. Rev. Lett.* **78** (1997) 1904-1907.

[45] A. Chekhlov and V. Yakhot, *Phys. Rev. E* **52** (1995) 5681-5684.

[46] A.M. Polyakov, *Phys. Rev. E* **52** (1995) 6183-6188.

[47] S.A. Boldyrev, *Phys. Rev. E* **55** (1997) 6907-6910.

[48] T. Gotoh and R.H. Kraichnan, *Phys. Fluids* **10** (1998) 2859-2866.

[49] R.H. Kraichnan, *Phys. Fluids* **11** (1999) 3738-3742.

[50] W. E and E. Vanden Eijnden, *Phys. Rev. Lett.* **83** (1999) 2572-2575.

[51] W. E and E. Vanden Eijnden, *Comm. Pure Appl. Math.* **53** (2000) 852-901.

[52] J. Bec and U. Frisch, *Phys. Rev. E* **61** (2000) 1395-1402.

[53] U. Frisch, J. Bec and B. Villone, *Physica D* (2000) (in press), cond-mat/9912110.

[54] J.V. José and E.J. Saletan, *Classical Dynamics: A Contemporary Approach* (Cambridge University Press, Cambridge, 1998).

[55] S. Aubry, *Physica D* **7** (1983) 240-258.

[56] J.N. Mather, *Topology* **21** (1982) 457-467.

[57] O. Oleinik, *Uspekhi Mat. Nauk* **12** (1957) 3-73. (*Russ. Math. Survey, Amer. Math. Transl. Series 2* **26**, 95-172.)

[58] W. E, K. Khanin, A. Mazel and Ya. Sinai, *Ann. Math.* **151** (2000) 877-960.

[59] T. Kontorova and Y.I. Frenkel, *Zh. Eskp. & Teor. Fiz.* **8** (1938) 1340.

[60] H.R. Jauslin, H.O. Kreiss and J. Moser, *Proc. Symp. Pure Math.* **65** (1999) 133-153.

[61] W. E, *Comm. Pure Appl. Math.* **52** (1999) 811-828.

[62] A.N. Sobolevski, *Sbornik Math.* **190** (1999) 1487-1504.